Stiffness prediction of CFRP/steel double strap joints

Yiyan Lu[1], Weijie Li[1, 2], Elyas Ghafoori [2], Hongjun Liang[3, 1] and Zhenzhen Liu[1]

[1] Wuhan University, Wuhan City, China
[2] Swiss Federal Laboratories for Materials Science and Technology (Empa), Dübendorf, Switzerland
[3] Huazhong University of Science and Technology, Wuhan City, China

ABSTRACT: Carbon fiber-reinforced polymer (CFRP) composites have been increasingly used in the strengthening and rehabilitation of steel structures. One area that receives much research interest is the adhesively bonded CFRP/steel joint, which simulates the cases of connecting two steel plates or strengthening cracked steel members with CFRP composites. Joint stiffness is an effective parameter in assessing the damage of structural elements. However, so far, only a few studies have focused on the prediction of CFRP/steel joint stiffness. The current study presents a stiffness prediction model for CFRP/steel double strap joints. Compared with an existing similar model, a more detailed mechanical analysis in the overlap region was conducted in the present model. The prediction results agreed well with the existing experimental data in the literature. Finally, the model was used to perform a parametric analysis.

1 INTRODUCTION

Carbon fiber-reinforced polymer (CFRP) composites, due to their high strength, good durability, flexibility in shape, ease of construction and excellent fatigue life, have been increasingly used in strengthening and rehabilitation of steel structures (Hollaway, 2010; Teng et al., 2012; Zhao and Zhang, 2007). It has been shown in previous studies that application of a CFRP composites to structural steel members can enhance their flexural capacity (Ghafoori and Motavalli 2013), buckling strength (Ghafoori and Motavalli 2015a & b) and fatigue behaviour (Ghafoori et al. 2015a, Ghafoori et al. 2015b, Ghafoori et al. 2015c). Adhesively-bonded CFRP/steel joint system has received considerable research attention. In such system, CFRP composites are used to connect two steel plates or to strengthen cracked steel members (Lam et al., 2007; Zhao and Zhang, 2007). Figure 1 presents a schematic view of CFRP/steel double strap joint.

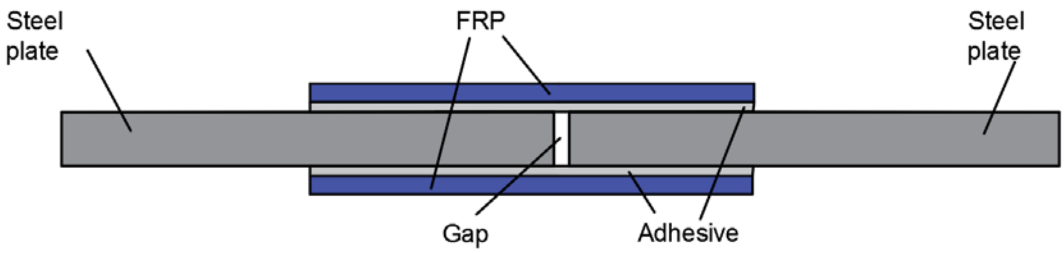

Figure 1. Schematic view of CFRP/steel double strap joint.

The majority of the studies on this topic have so far only focused on interface behavior of joints, e.g. the bond slip model, the shear stress or strain distribution, and the joint strength prediction (Al-Zubaidy et al., 2012; Nguyen et al., 2013; Wu et al., 2012; Yu et al., 2012), while the prediction of CFRP/steel joint stiffness, which is the slope of load-displacement curves, have not been much studied. Ghafoori et al. (2012a, 2012b) have studied experimentally the effect of CFRP strengthening of cracked steel beams on their load-displacement (i.e., stiffness) behavior. The results have shown that that application of the pre-stressed CFRP plates could effectively increase the stiffness of the steel beam by applying a compressive stress to the cracked section, and, therefore increasing the net cross-section. Hosseini et al. (2017) have also shown that CFRP laminates could be used for strengthening of cracked steel plates. Owens and Lee-Sullivan (2000a; 2000b) have studied the stiffness behavior of composite/aluminum joints. Although their stiffness prediction model has been validated by experimental data, it involves the Adams-Peppiatt stress distribution formula, which requires the division of overlap region into many small parts and is a complex technique. Xiao et al. (2004) have proposed a much simpler model (denoted as the Xiao model), which was later adopted by Deb et al. (2008). Their model assumes that the tensile stress in the overlap region decreases linearly from maximum value at the loading end to zero at the free end. Their assumption provides an insight into the analysis of CFRP/steel joints. However, as their joints were metal/metal joints with a bond length of only 25 mm, and the bond length of CFRP/steel joints might reach as long as 100 mm (Wu et al. 2012), the Xiao model might be inaccurate for the analysis the CFRP/steel joints.

The stiffness of joints is an excellent non-destructive parameter in monitoring the damage of structural elements and assessing the residual life (O'Brien, 1980; Owens and Lee-Sullivan, 2000a). In addition, an accurate analysis of the stiffness contributes to a better understanding of the mechanical behavior of joints under tensile load.

This paper aims at developing an accurate stiffness prediction model for CFRP/steel double strap joints. The proposed model was based on the Xiao model, but a more detailed tensile stress analysis within the bond region was conducted. The prediction results were compared with the existing experimental data in the literature. At the end, the verified model was used to perform a parametric analysis.

2 STIFFNESS PREDICTION MODEL

In this section, first, the analysis of double lap joints is presented. This is because the double strap joint could be deemed as a combination of two double lap joints, which results in an easier analysis process. The stiffness prediction models of symmetrical double strap joints (where bond lengths of the two double lap joints are the same) and unsymmetrical double strap joints (where the bond lengths of the double lap joints are different) will be also presented at the end of this section.

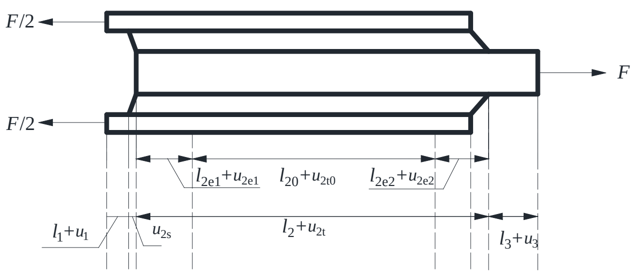

Figure 2. Schematic view of CFRP/steel double lap joint.

The double lap joint is divided into the following regions: double leg region (length= l_1), overlap region (length= l_2), and single leg region (length= l_3), as shown in Figure 2.

(1) Double leg region (length= l_1)

The strain and displacement of the double leg region l_1 , ε_1 and u_1 , are as follows:

$$\varepsilon_1 = \frac{\sigma}{E_{\mathrm{frp}}} = \frac{F}{2bt_{\mathrm{frp}}E_{\mathrm{frp}}} \tag{1}$$

$$u_1 = \frac{Fl_1}{2bt_{\mathrm{frp}}E_{\mathrm{frp}}} \tag{2}$$

where F is the tensile load and b is the width of joint. Furthermore t_{frp} and E_{frp} are the thickness and elastic modulus of FRP composites, respectively.

(2) Overlap region (length= l_2)

The displacement of the overlap region l_2 , u_2 , consists of two parts, i.e. the adhesive shear deformation part $u_{2\mathrm{s}}$ and the steel tensile part $u_{2\mathrm{t}}$. The calculation of $u_{2\mathrm{s}}$ and $u_{2\mathrm{t}}$ depends on whether l_2 is larger than the effective bond length l_{e} . The effective bond length is the bond length which the ultimate load does not increase with any further increase in it. l_{e} could be calculated according to the model proposed by Hart-Smith (1973):

$$l_{\mathrm{e}} = \frac{P_{\mathrm{u}}}{2\tau_{\mathrm{p}}b} + \frac{2}{\sqrt{\dfrac{G_{\mathrm{a}}}{t_{\mathrm{a}}}\left(\dfrac{1}{E_{\mathrm{frp}}t_{\mathrm{frp}}} + \dfrac{2}{E_{\mathrm{s}}t_{\mathrm{s}}}\right)}} \tag{3}$$

where t_{a} and G_{a} are the thickness and shear modulus of the bonding adhesive, respectively. t_{s} and E_{s} are the thickness and elastic modulus of steel, respectively. τ_{p} is the shear strength of the bonding adhesive. P_{u} is the lesser of P_{i} and P_{o} :

$$P_{\mathrm{i}} = b\sqrt{\left[2\tau_{\mathrm{p}}t_{\mathrm{a}}\left(\frac{1}{2}\gamma_{\mathrm{e}} + \gamma_{\mathrm{p}}\right)\right] \bullet 2E_{\mathrm{s}}t_{\mathrm{s}}\left(1 + \frac{E_{\mathrm{s}}t_{\mathrm{s}}}{2E_{\mathrm{frp}}t_{\mathrm{frp}}}\right)} \tag{4}$$

$$P_{\mathrm{o}} = b\sqrt{\left[2\tau_{\mathrm{p}}t_{\mathrm{a}}\left(\frac{1}{2}\gamma_{\mathrm{e}} + \gamma_{\mathrm{p}}\right)\right] \bullet 4E_{\mathrm{frp}}t_{\mathrm{frp}}\left(1 + \frac{2E_{\mathrm{frp}}t_{\mathrm{frp}}}{E_{\mathrm{s}}t_{\mathrm{s}}}\right)} \tag{5}$$

where P_{i} and P_{o} represent the ultimate load when $E_{\mathrm{s}}t_{\mathrm{s}} < 2E_{\mathrm{frp}}t_{\mathrm{frp}}$ and $E_{\mathrm{s}}t_{\mathrm{s}} \geq 2E_{\mathrm{frp}}t_{\mathrm{frp}}$, respectively. γ_{e} and γ_{p} are the elastic shear strain and plastic shear strain of the bonding adhesive, respectively. The relationship between γ_{p} and γ_{e} could be assumed as $\gamma_{\mathrm{p}} = 5\gamma_{\mathrm{e}}$ according to the suggestion of Wu et al. (2012).

For joints with l_2 less than l_e, it can be simply assumed that the tensile stress of the steel decreases linearly to zero along the bond length. Therefore, u_{2s} and u_{2t} could be respectively calculated as follows:

$$u_{2s} = \gamma_a t_a = \frac{\tau_{ave}}{G_a} t_a = \frac{F t_a}{2 b l_2 G_a} \quad (6)$$

$$u_{2t} = \frac{F l_2}{2 b t_s E_s} \quad (7)$$

For joints with l_2 equal to or larger than l_e, l_2 is subdivided into l_{2e1}, l_{2e2} and l_{20}. The sum of l_{2e1} and l_{2e2} is l_e, i.e.:

$$l_2 = l_{2e1} + l_{2e2} + l_{20} = l_e + l_{20} \quad (8)$$

Within l_e, the assumption of linear change in tensile stress of adherends could be adopted. Within l_{20}, however, the outer adherend (CFRP) and inner adherend (steel) are of the same constant nonzero tensile strain.

Therefore, u_{2s} is:

$$u_{2s} = \gamma_a t_a = \frac{\tau_{ave}}{G_a} t_a = \frac{F t_a}{2 b l_e G_a} \quad (9)$$

u_{2t} is composed of tensile deformations in l_{2e1}, l_{2e2} and l_{20}, which are u_{2e1}, u_{2e2}, and u_{2t0}, respectively. $u_{2e1} + u_{2e2}$ is calculated as follows:

$$u_{2e1} + u_{2e2} = \frac{F(l_{2e1} + l_{2e2})}{2 b t_s E_s} = \frac{F l_e}{2 b t_s E_s} \quad (10)$$

The calculation of u_{2t0} depends upon the tensile strain ε. As the load F is distributed between CFRP and steel based on their respective stiffness, F is expressed as follows:

$$F = 2 b t_{frp} E_{frp} \varepsilon + b t_s E_s \varepsilon \quad (11)$$

By transforming equation (11), the strain ε is:

$$\varepsilon = \frac{F}{2 b t_{frp} E_{frp} + b t_s E_s} \quad (12)$$

As ε is also equal to u_{2t0} / l_{20}, u_{2t0} is derived as:

$$u_{2t0} = \frac{F l_{20}}{2 b t_{frp} E_{frp} + b t_s E_s} \quad (13)$$

Based on equations (10) and (13), the displacement u_{2t} is:

$$u_{2t} = u_{2e1} + u_{2e2} + u_{2t0} = \frac{F l_e}{2 b t_s E_s} + \frac{F l_{20}}{2 b t_{frp} E_{frp} + b t_s E_s} \quad (14)$$

Therefore for joints with l_2 less than l_e, the displacement u_2 is:

$$u_2 = u_{2s} + u_{2t} = \frac{Ft_a}{2bl_2G_a} + \frac{Fl_2}{2bt_sE_s} \tag{15}$$

and for joints with l_2 equal to or larger than l_e, the displacement u_2 is:

$$u_2 = u_{2s} + u_{2t} = \frac{Ft_a}{2bl_eG_a} + \frac{Fl_e}{2bt_sE_s} + \frac{Fl_{20}}{2bt_{frp}E_{frp} + bt_sE_s} \tag{16}$$

It is worth mentioning that although the deformation of CFRP in the overlap region was not expressed explicitly by formula, the deformation of CFRP was taken into account. In region l_{20}, CFRP and steel have the same tensile deformation. In l_{2e1} and l_{2e2}, the difference between deformation of CFRP and that of steel is reflected in the adhesive shear deformation.

(3) Single leg region (length=l_3)

$$u_3 = \frac{Fl_3}{bt_sE_s} \tag{17}$$

By adding up u_1, u_2, and u_3, the total displacement u of the double lap joint is derived:

$$u = u_1 + u_2 + u_3 = \begin{cases} \dfrac{Fl_1}{2bt_{frp}E_{frp}} + \dfrac{Ft_a}{2bl_2G_a} + \dfrac{Fl_2}{2bt_sE_s} + \dfrac{Fl_3}{bt_sE_s} \ (\text{for } l_2 < l_e) \\ \dfrac{Fl_1}{2bt_{frp}E_{frp}} + \dfrac{Ft_a}{2bl_eG_a} + \dfrac{Fl_e}{2bt_sE_s} + \dfrac{F(l_2 - l_e)}{2bt_{frp}E_{frp} + bt_sE_s} + \dfrac{Fl_3}{bt_sE_s} \ (\text{for } l_2 \geq l_e) \end{cases} \tag{18}$$

Therefore the stiffness for double lap joints is:

$$K_{lap} = \frac{F}{u} = \begin{cases} 1/(\dfrac{l_1}{2bt_{frp}E_{frp}} + \dfrac{t_a}{2bl_2G_a} + \dfrac{l_2}{2bt_sE_s} + \dfrac{l_3}{bt_sE_s}) \ (\text{for } l_2 < l_e) \\ 1/(\dfrac{l_1}{2bt_{frp}E_{frp}} + \dfrac{t_a}{2bl_eG_a} + \dfrac{l_e}{2bt_sE_s} + \dfrac{(l_2 - l_e)}{2bt_{frp}E_{frp} + bt_sE_s} + \dfrac{l_3}{bt_sE_s}) \ (\text{for } l_2 \geq l_e) \end{cases} \tag{19}$$

For symmetrical double strap joints, the joint stiffness is half of the value of the double lap joints:

$$K_{sym\text{-}strap} = \frac{K_{lap}}{2} \tag{20}$$

For unsymmetrical double strap joints, the joint stiffness is:

$$K_{unsym\text{-}strap} = \frac{1}{\dfrac{1}{K_{lap1}} + \dfrac{1}{K_{lap2}}} \tag{21}$$

where K_{lap1} and K_{lap2} are the joint stiffness of the two double lap joints which constitute the double strap joint.

3 VALIDATION OF THE MODEL

The prediction results are compared with the experimental data from literature, as shown in Table 1, together with the predictions from the Xiao model. The average estimated errors relative to the experimental values of the proposed model and the Xiao model are 0.13 and 0.21, respectively, indicating the accuracy of the proposed model. The existing errors might be due to the assumption in adherend tensile stress distribution.

Table 1. Comparison of the existing experimental and theoretical studies and the proposed model

Set	Specimen	Experimental K_{exp} (kN/mm)	Theoretical (this model)		Theoretical (the Xiao Model)	
			K_{theo} (kN/mm)	K_{theo} / K_{exp}	K_{theo} (kN/mm)	K_{theo} / K_{exp}
Nguyen et al. (2011)	CF1-BL60-T20	132.8	144.7	1.09	177.7	1.34
	CF3-BL100-T20	183.3	170.2	0.93	209.1	1.14
Lam et al. (2007)	P-2-50-1/2	192.8	223.0	1.16	223	1.16
	P-2-100-1/2	195.9	239.5	1.22	249.3	1.27
	P-2-150-1/2	203.1	252.1	1.24	277.3	1.37
	P-3-50-1/4	122.8	113.4	0.92	113.4	0.92
	P-3-100-1/4	133.8	125.4	0.94	125.5	0.94
	P-3-150-1/4	148.2	139.1	0.94	139.4	0.94
Matta et al. (2005)	DSS (unfatigued)	65.1	75.0	1.15	94.7	1.45

4 PARAMETRIC ANALYSIS

A parametric analysis was conducted using the proposed stiffness prediction model. The parameters investigated in the present paper were bond length and adherend stiffness ratio, the latter of which is defined as $2E_{frp}t_{frp} / E_s t_s$ (Lam et al., 2007). The data of joint geometry and material properties were of joint P-3-50-1/4 from Lam et al. (2007). The geometry and material properties are as follows: $l_1 = 1\text{mm}$, $l_2 = 49\text{mm}$, $l_3 = 251\text{mm}$, $t_{frp} = 3.66\text{mm}$, $E_{frp} = 176061\text{MPa}$, $t_s = 6.09\text{mm}$, $E_s = 205700\text{MPa}$, $t_a = 0.65\text{mm}$, and $G_a = 1680\text{MPa}$.

Figure 3 shows the effect of bond length on stiffness of CFRP/steel double strap joints, with the bond length ranging from 10 to 290 mm. It could be observed that the joint stiffness increases almost linearly with the increase in bond length, which can be also seen in the experimental results. The effects of bond length for joints with other configurations (e.g., the total length of joint, the adherend stiffness ratio, etc.) require further investigation.

Figure 4 shows the effect of adherend stiffness ratio on stiffness of CFRP/steel double strap joints, with the value of adherend stiffness ratio ranging from 0.01 to 1.00. The increase in adherend stiffness ratio was realized by increasing the elastic modulus of the CFRP composite. It can be seem from Figure 4 that the joint stiffness increases substantially when the adherend stiffness ratio increases from 0.01 to about 0.1. From 0.1 to about 0.25, the increase in stiffness is not substantial. From 0.25 to 1.0, the stiffness is almost constant. Further investigation into the component deformation of each part shows that the change of stiffness is a result of deformation $u_1 = \frac{Fl_1}{2bt_{frp}E_{frp}}$ in the double leg region, which is an inverse proportional function of E_{frp}, and, therefore leading to the insensitivity to changes of E_{frp} when E_{frp} is rather large.

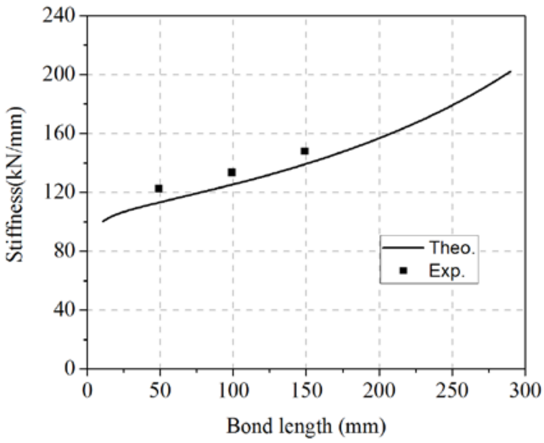

Figure 3. Effect of bond length on stiffness.

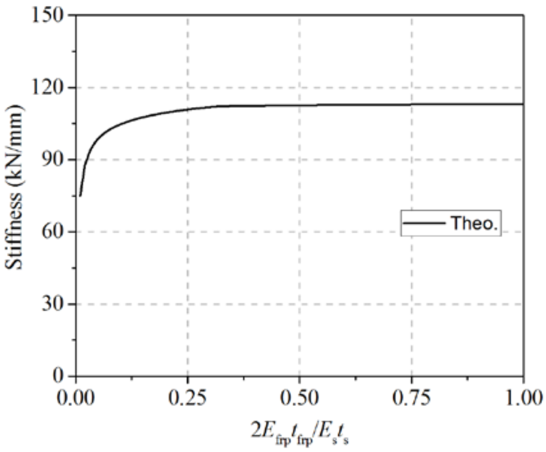

Figure 4. Effect of adherend stiffness ratio on stiffness.

5 CONCLUSIONS

A stiffness prediction model for double strap joints under tensile load was presented in this paper. The results of the model agreed well with the existing experimental data in the literature. Based on the presented model, a parametric analysis was conducted. It was observed that the stiffness increases almost linearly with an increase in the bond length, and a substantial increase in stiffness occurs when the adherend stiffness ratio increases from 0.01 to about 0.1.

ACKNOWLEDGMENTS

The authors wish to acknowledge the fund from Chinese Scholarship Council (201606270106).

REFERENCES

Al-Zubaidy, H., Al-Mahaidi, R. and Zhao, X.-L., 2012. Experimental investigation of bond characteristics between CFRP fabrics and steel plate joints under impact tensile loads. *Composite Structures*, 94(2): 510-518.

Deb, A., Malvade, I., Biswas, P. and Schroeder, J., 2008. An experimental and analytical study of the mechanical behaviour of adhesively bonded joints for variable extension rates and temperatures. *International Journal of Adhesion and Adhesives*, 28(1-2): 1-15.

Ghafoori, E. & Motavalli, M. 2013. Flexural and interfacial behavior of metallic beams strengthened by prestressed bonded plates. *Composite Structures,* 101(15)**,** 22-34.

Ghafoori, E. & Motavalli, M. 2015a. Lateral-torsional buckling of steel I-beams retrofitted by bonded and un-bonded CFRP laminates with different pre-stress levels: experimental and numerical study. *Construction and Building Materials,* 76(76)**,** 194–206.

Ghafoori, E. & Motavalli, M. 2015b. Normal, high and ultra-high modulus CFRP laminates for bonded and un-bonded strengthening of steel beams. *Materials and Design*, 67**,** 232–243.

Ghafoori, E., Motavalli, M., Botsis, J., Herwig, A. & Galli, M. 2012a. Fatigue strengthening of damaged metallic beams using prestressed unbonded and bonded CFRP plates. *International Journal of Fatigue,* 44(2)**,** 303-315.

Ghafoori, E., Motavalli, M., Nussbaumer, A., Herwig, A., Prinz, G. & Fontana, M. 2015a. Determination of minimum CFRP pre-stress levels for fatigue crack prevention in retrofitted metallic beams. *Engineering Structures,* 84(10)**,** 29–41.

Ghafoori, E., Motavalli, M., Nussbaumer, A., Herwig, A., Prinz, G. S. & Fontana, M. 2015b. Design criterion for fatigue strengthening of riveted beams in a 120-year-old railway metallic bridge using pre-stressed CFRP plates. *Composites Part B: Engineering,* 68**,** 1-13.

Ghafoori, E., Motavalli, M., Zhao, X. L., Nussbaumer, A. & Fontana, M. 2015c. Fatigue design criteria for strengthening metallic beams with bonded CFRP plates. *Engineering Structures,* 101**,** 542-557.

Ghafoori, E., Schumacher, A. & Motavalli, M. 2012b. Fatigue behavior of notched steel beams reinforced with bonded CFRP plates: Determination of prestressing level for crack arrest. *Engineering Structures,* 45(15)**,** 270-283.

Hart-Smith, L.J., 1973. Adhesive-bonded double-lap joints. *International Journal of Solids & Structures*, 31(21): 2919-2931.

Hollaway, L.C., 2010. A review of the present and future utilisation of FRP composites in the civil infrastructure with reference to their important in-service properties. *Construction and Building Materials*, 24(12): 2419-2445.

Hosseini, A., Ghafoori, E., Motavalli, M., Nussbaumer, A. & Zhao, X.-L. 2017. Mode I Fatigue Crack Arrest in Tensile Steel Members Using Prestressed CFRP Plates. *Composite Structures,* DOI: doi.org/10.1016/j.compstruct.2017.06.056.

Lam, A.C.C., Cheng, J.J.R., Yam, M.C.H. and Kennedy, G.D., 2007. Repair of steel structures by bonded carbon fibre reinforced polymer patching: experimental and numerical study of carbon fibre reinforced polymer – steel double-lap joints under tensile loading. *Canadian Journal of Civil Engineering*, 34(12): 1542-1553.

Matta, F., Karbhari, V.M. and Vitaliani, R., 2005. Tensile response of steel/CFRP adhesive bonds for the rehabilitation of civil structures. *Structural Engineering and Mechanics*, 20(5): 589-608.

Nguyen, T.-C., Bai, Y., Zhao, X.-L. and Al-Mahaidi, R., 2011. Mechanical characterization of steel/CFRP double strap joints at elevated temperatures. *Composite Structures*, 93(6): 1604-1612.

Nguyen, T.-C., Bai, Y., Zhao, X.-L. and Al-Mahaidi, R., 2013. Curing effects on steel/CFRP double strap joints under combined mechanical load, temperature and humidity. *Construction and Building Materials*, 40: 899-907.

O'Brien, T.K., 1980. Stiffness change as a nondestructive damage measurement, *Mechanics of nondestructive testing*. Springer, pp. 101-121.

Owens, J.F. and Lee-Sullivan, P., 2000a. Stiffness behaviour due to fracture in adhesively bonded composite-to-aluminum joints I. Theoretical model. *International journal of adhesion and adhesives*, 20(1): 39-45.

Owens, J.F. and Lee-Sullivan, P., 2000b. Stiffness behaviour due to fracture in adhesively bonded composite-to-aluminum joints II. Experimental. *International journal of adhesion and adhesives*, 20(1): 47-58.

Teng, J.G., Yu, T. and Fernando, D., 2012. Strengthening of steel structures with fiber-reinforced polymer composites. *Journal of Constructional Steel Research*, 78: 131-143.

Wu, C., Zhao, X., Hui Duan, W. and Al-Mahaidi, R., 2012. Bond characteristics between ultra high modulus CFRP laminates and steel. *Thin-Walled Structures*, 51: 147-157.

Xiao, X., Foss, P.H. and Schroeder, J.A., 2004. Stiffness prediction of the double lap shear joint. Part1: Analytical solution. *International Journal of Adhesion and Adhesives*, 24(3): 229-237.

Yu, T., Fernando, D., Teng, J.G. and Zhao, X.L., 2012. Experimental study on CFRP-to-steel bonded interfaces. *Composites Part B: Engineering*, 43(5): 2279-2289.

Zhao, X.-L. and Zhang, L., 2007. State-of-the-art review on FRP strengthened steel structures. *Engineering Structures*, 29(8): 1808-1823.